

OPTIMIZATION OF DIVERGING SECTION OF PUTNAM NOZZLE AT DIFFERENT CONICAL ANGLE

METE ATASOY^{*}, MEHMET A. ELDEMIR^{*} AND TEZCAN UNLU^{*}

^{*} Roketsan Missile Inc.

Kemalpaşa Mahallesi Sehit Yuzbasi Adem Kutlu Sokak No: 21
06780 Ankara, TURKEY

E-mail: mete.atasoy@roketan.com.tr, mehmet.eldemir@roketan.com.tr,
tezcan.unlu@roketan.com.tr - web page: <http://www.roketan.com.tr>

Key words: Putnam Nozzle, Plume, Nozzle Dynamic, Optimization.

Summary. *This article includes the optimization of Putnam Nozzle with the method of Genetic Algorithm. The diverging section of conical angle and base thickness in a certain limit are optimized by maximizing nozzle performance. A numerical method of modelling for exhaust plume is based on 2-equation realizable k-epsilon turbulence model with 2nd Order Discretization and Density-Based at a steady state. The nozzle model for validation is taken from⁷ where experimental measurement of exhaust velocity and pressure has been carried out. Generic model is created in ANSYS Design Modeler and meshed with quad elements in ANSYS Mesher. Then, optimization algorithm is used in the Design Modeler software to lead best configuration by changing conical angle (α) and aft angle (β). ANSYS FLUENT v19.3 is chosen to be flow solver for N-S equation to imply. After having numerical results best agreement with the experimental data, optimum configuration that has maximum thrust value and minimum drag is achieved. In addition, the effects of divergent section's angle and radius on thrust and drag performance are examined. Results are compared with each other to show how geometry input parameters are sensitive to performance parameter.*

1 INTRODUCTION

Propulsion system in aviation technology has challenging requirements to fulfill, high precision of thrust. All turbine engines have nozzle parts, simple device with extremely hot section. In order to model nozzle, mathematical aspects should be carefully understood due to slight change in the flow characteristics at the rear part. That interaction effects airflow around the air vehicle, leading total drag penalties. Most supersonic aircraft use a converging-diverging nozzle. The physics behind it had been investigated and implementation of equations for nozzle dynamics had been raised with exploration of supercomputers.

High fluid flow with little friction loss at the nozzle, the isentropic models consider as an acceptable methodology for preliminary design stage. Computational Fluid Dynamics is the best available analysis tool to simulate nozzle flow. The numerical solver gives fairly well approach for such cases, but numerical method has to be chosen carefully since sudden temperature change in fluid. When computational cost and accuracy considered, RANS-based turbulence models give good trade-off.

This paper describes the optimization of nozzle geometry with the method of 2-equation k-epsilon turbulence model to carry out the preliminary design. Optimization with CFD analysis consists of test condition to validate, optimize the nozzle geometry with genetic algorithm and performance calculation to examine. Exhaust radius, boat-tail length and boat-tail angle are parameters to change for optimization. The numerical results were investigated with respect to nozzle performance and optimum drag level.

2 METHODOLOGY

A converging-diverging nozzle is modelled under the assumption of isentropic flow and perfect gas model. To model DC nozzle, Navier-Stokes equations are used to find conservative values in the domain.

2.1 Nozzle flow equation

Conservation of mass, momentum and energy in terms of Mach number become:

$$\frac{dp}{p} - \frac{dT}{2T} + \frac{dM}{M} + \frac{dA}{A} = 0 \quad (1)$$

$$\frac{dv^2}{2} - dh - Tds = 0 \quad (2)$$

$$(1 - M^2) \frac{dv}{v} = - \frac{dA}{A} \quad (3)$$

where A represent cross-section area of the duct.

Choked flow is a compressible flow effect that does not depend on the back pressure.

3 DISCUSSION AND RESULTS

3.1 Numerical validation

In this article, Putnam Nozzle Model⁷ was used to validate our numerical approach. Model is sketch as follows,

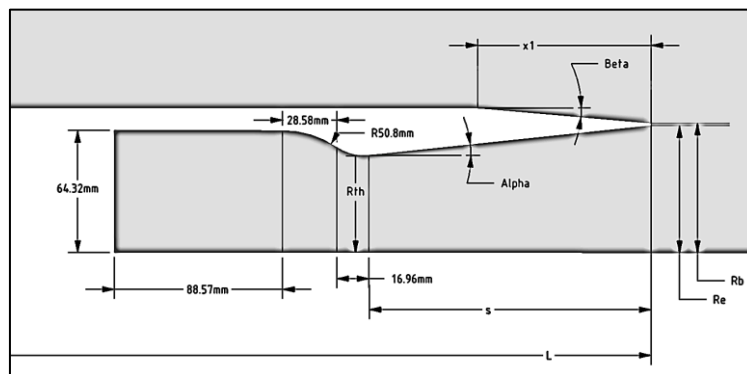


Figure 1: Putnam Nozzle Geometry Parameters

Alpha (°)	beta (°)	x ₁ (mm)	L (mm)	s (mm)	R _{th} (mm)	Re(mm)	Rb(mm)
6.04	5	91.09	1132.49	151.05	51.115	66.96	68.23

Table 1: Model Parameters Length for Putnam Nozzle

All dimensions in Figure 1 are tabulated above table in mm.

To optimize nozzle divergence section, Alpha, base-thickness and boat-tail length(x₁) are used to manipulate to find better performance for nozzle section.

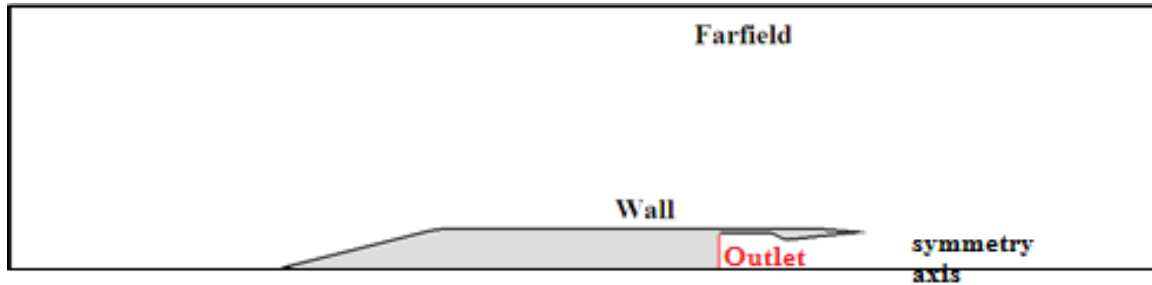


Figure 2 : Boundary Condition Types for CFD Analysis

Boundary Conditions are shown in Figure 2. Pressure Outlet (red) is specified with total temperature and total pressure to model exhaust flow. Flow direction, velocity and pressure are defined at the pressure far-field. The values taken from experiment⁷ detailed in Table 2 applied to numerical solver.

Static Ambient Pressure (Ps)	11606 Pa
Ambient Temperature (Ts)	161 K
Mach	2.2
Total Pressure @Nozzle Outlet	94241 Pa
Total Temperature @Nozzle Outlet	300 K

Table 2: Boundary Conditions for CFD Analysis

In order to achieve converged numerical solution, the elements are modeled in quad mesh. Figure 3 shows element structure, especially fine elements is set for those regions expected to high gradient in the conservative derivatives. It is known that quadrilateral meshes advantages are better convergence and higher resolutions.

3.1.1 Mesh convergence and CPU convergence

Number of mesh elements can affect analysis elapsed time. Especially, optimization requires a number of analyses to find better configuration. Numerical solver performs better with good quality elements in the control volume. Also, unnecessary mesh elements decelerate the solver. To avoid and to reduce the solution elapsed time, mesh convergence is done with different number of mesh elements.

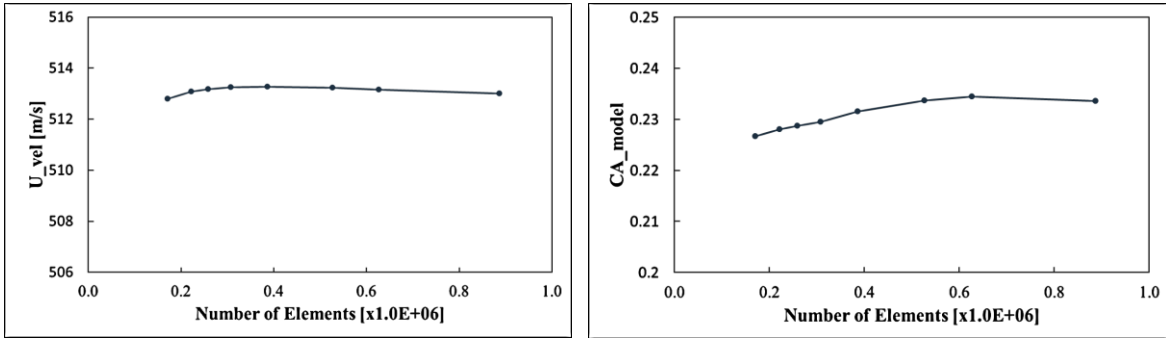


Figure 3: Grid Convergence Study for Putnam Nozzle

From the grid convergence study, axial force coefficients have steady state form when number of elements is $0.6E+06$. U_vel value represents the area weighted average velocity calculated from the nozzle exit and it converged when number of the elements is smaller.

Another factor that effects solution time is the parallelization types of solver. Open MP and MPI programming are used for high performance computing algorithms. The differences between Open MP and MPI is that Open MP is way to parallel on shared memory devices but MPI is based on parallel code over distributed system. ANSYS Fluent has 3 parallelization types to solve flow equations. Open MP, IBM MPI and INTEL MPI are used to examine their performance on solver.

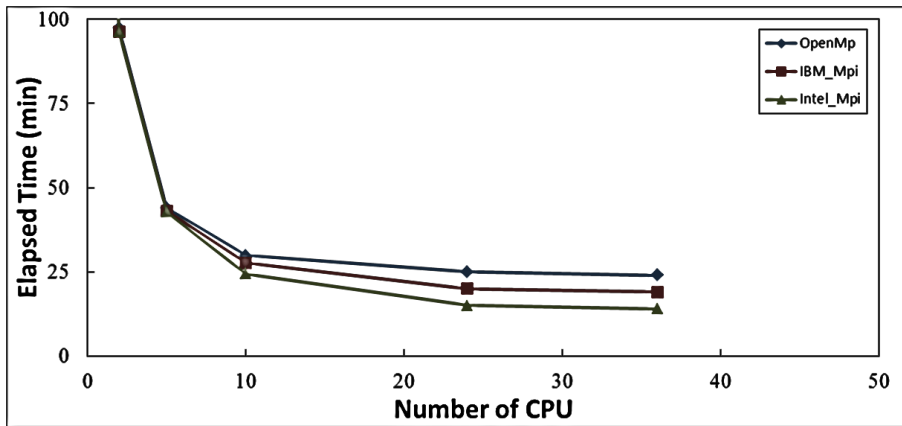


Figure 4: CPU Convergence with different parallelization type for Putnam Nozzle

Intel MPI has less elapsed time at the higher CPU. It has 20% less wall clock time than IBM MPI and 25% less wall clock time than Open MP when 24 CPU is used.

3.1.2 Comparison with experiments

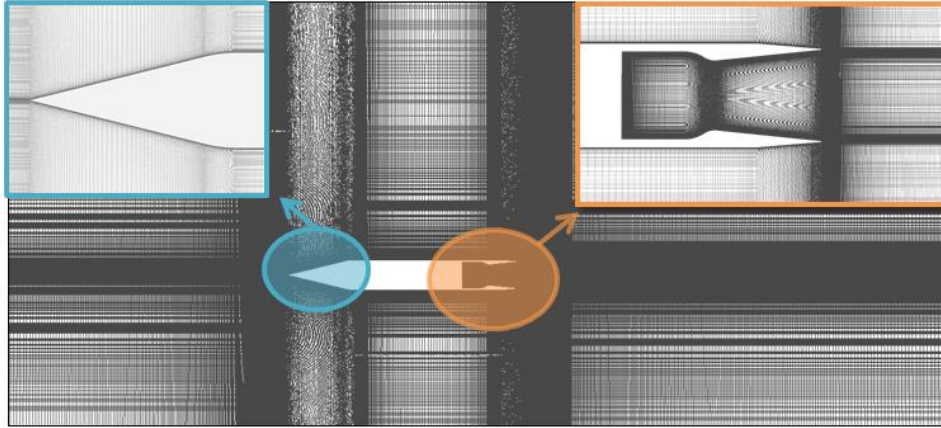


Figure 5: Fine Quad Elements for 2D Putnam Nozzle

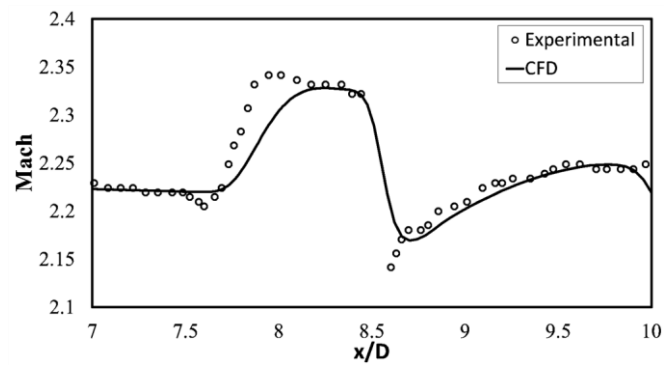


Figure 6: Variation in Mach number along the axis at a distance 152.4 mm above the centerline of Putnam nozzle

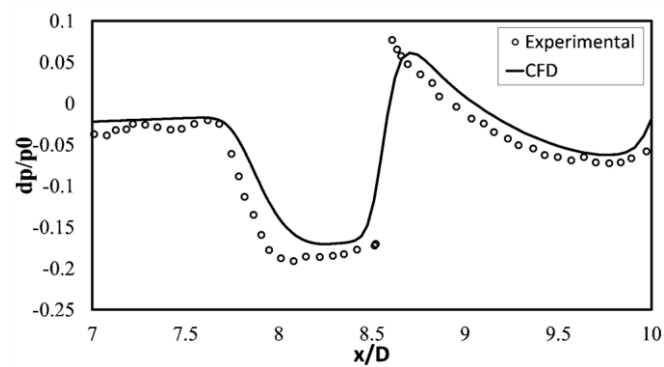


Figure 7: Variation in Pressure $\Delta P/P_0$ along the axis at a distance 152.4 mm above the centerline of Putnam nozzle

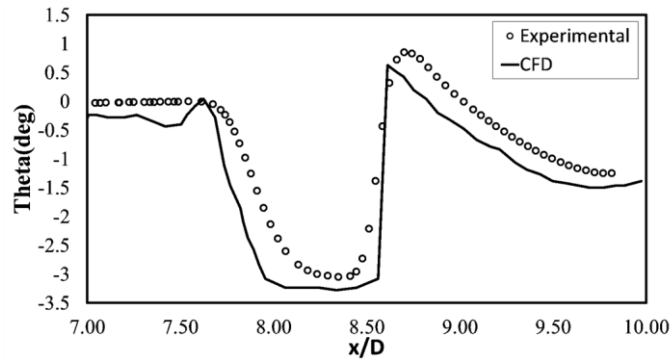


Figure 8: Variation in Flow Angle along the axis at a distance 152.4 mm above the centerline of Putnam nozzle

Comparison for validation data with Mach number at the rear part, pressure difference ratio free-stream pressure and flow angle with respect to position given figures above. To simulate optimization cycle, numerical results give us meaningful nozzle structure in the Figure 9 as well. For pressure ratio and flow angle, the values are smaller at some points, but numerical analysis capture the shock at the non-dimensional (x/D) distance of 8.5.

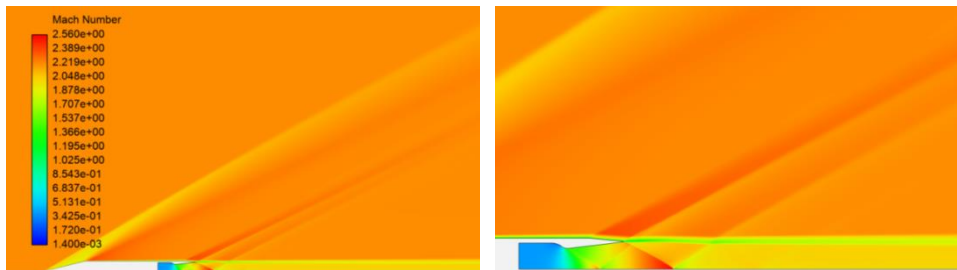


Figure 9 : Mach Contours with zoomed in Putnam Nozzle using $k-\epsilon$ Turbulence Model

3.2 Performance optimization

In this section, the methodology for optimization is shown in Figure 10. Optimization cycle includes model definition, mesh generation and numerical analysis. Input for Putnam nozzle divergence section consists of Beta (β), base thickness, boat-tail length. Constrains for geometrical sets shown in Table 3.

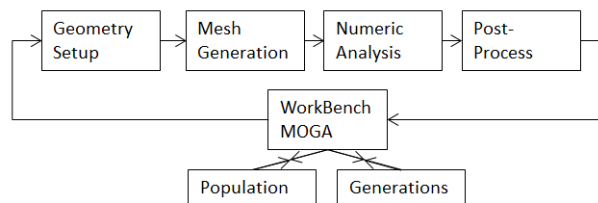


Figure 10: Multi-Objective Genetic Algorithm Structure for Nozzle Optimization

From the Figure 10, optimization procedure includes model generation, creating mesh

elements and numerical analysis. ANSYS Workbench has also optimization tool to let simple model analysis.

Parameter	Upper Limit	Baseline (Putnam Nozzle)	Lower Limit
Beta (deg)	195	185	175
Boat-tail Thickness(mm)	3	1.27	1
Boat-tail Length(mm)	120	91.09	60

Table 3 : Input Parameters Limitation

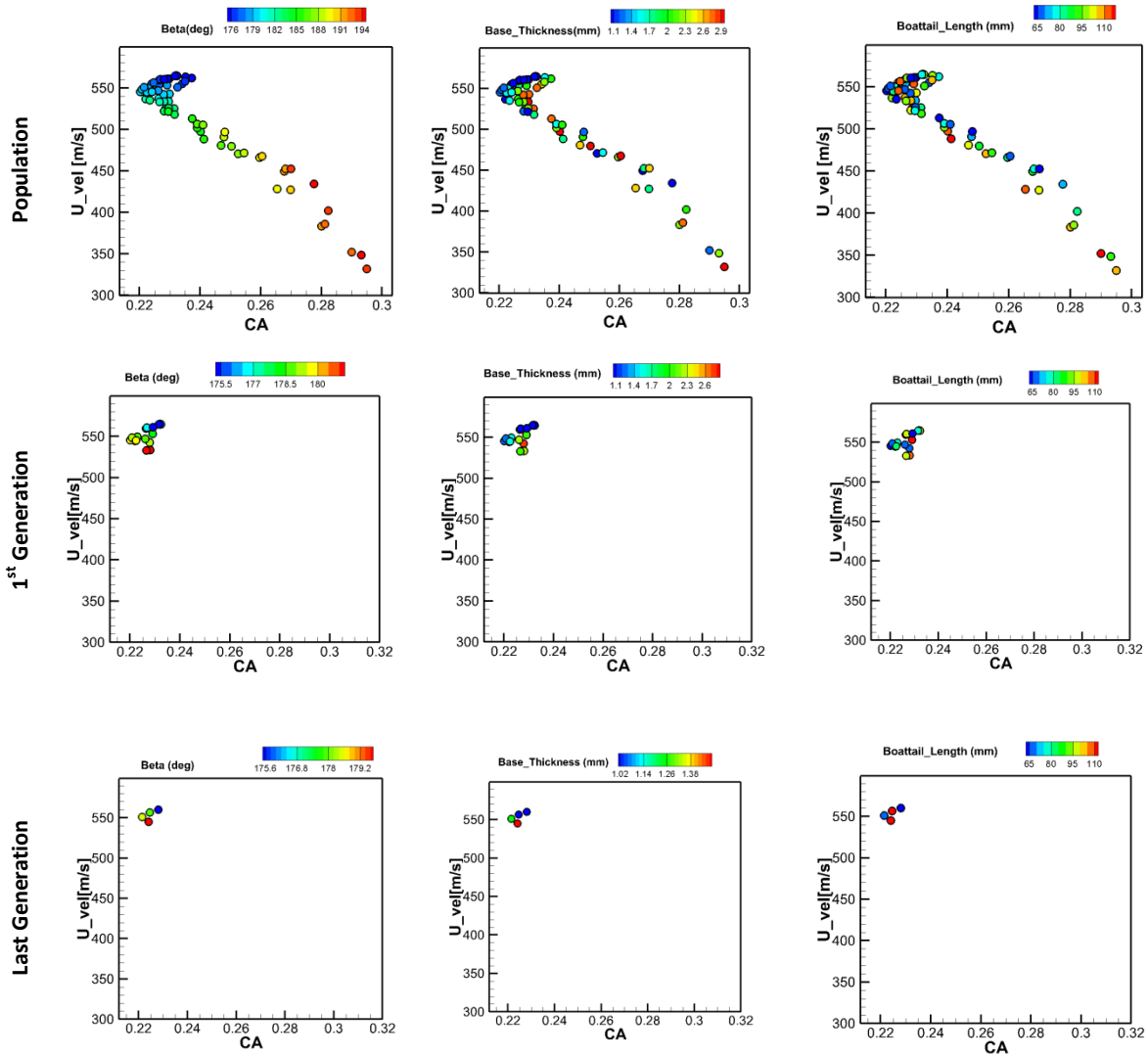


Figure 11: The Behavior of Input Parameters on Performance (2D view)

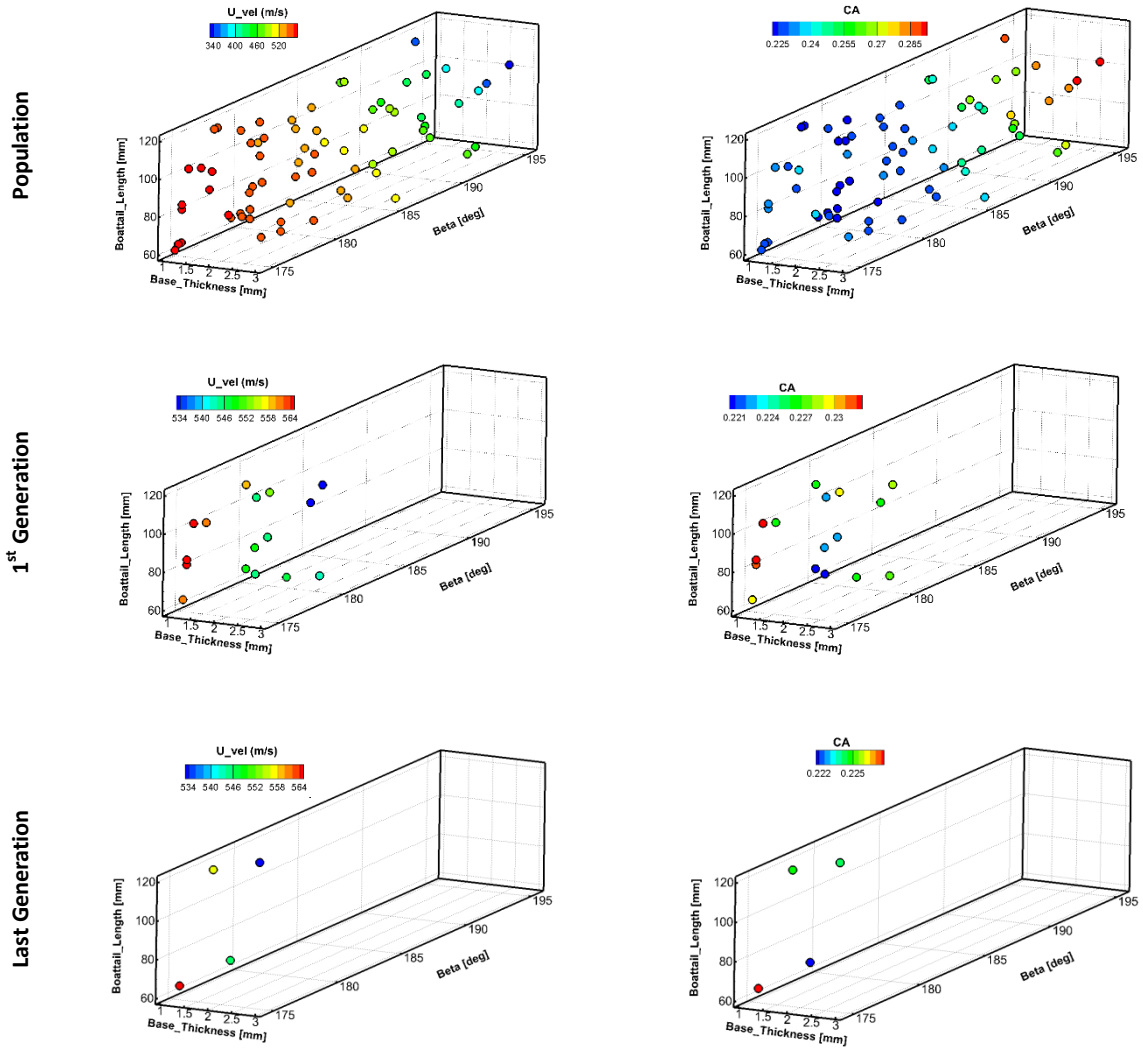


Figure 12: The Behavior of Input Parameters on Performance (3D view)

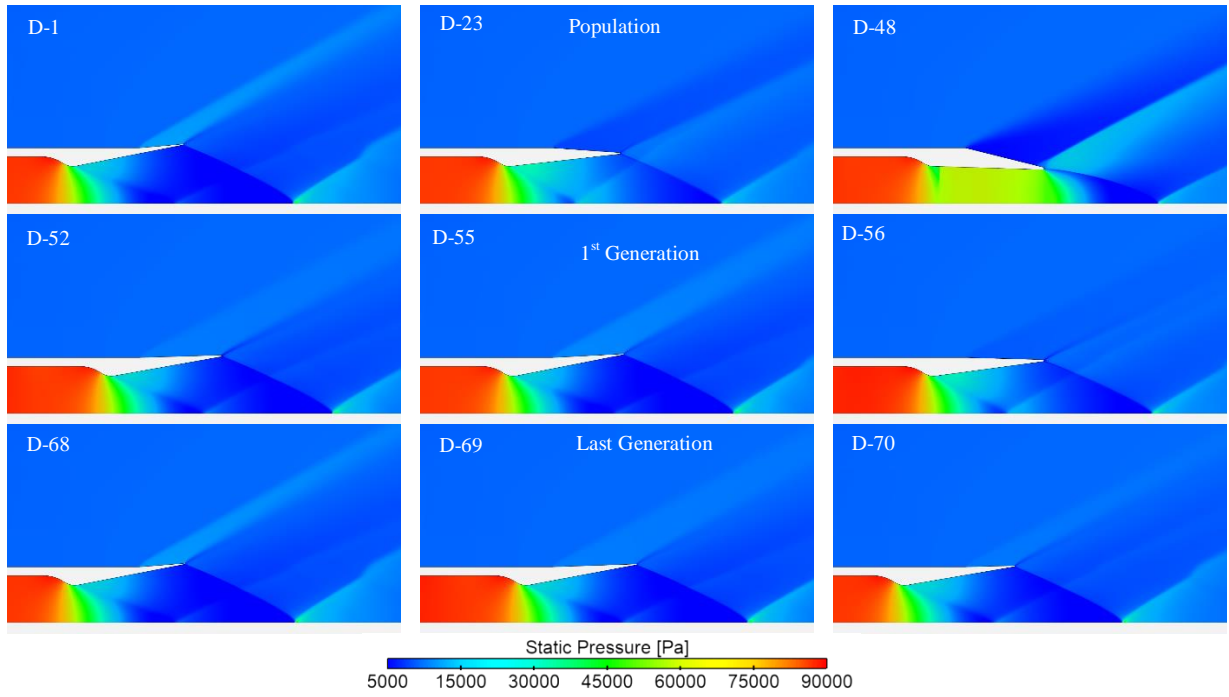


Figure 13: Static Pressure Contours for certain Design Points

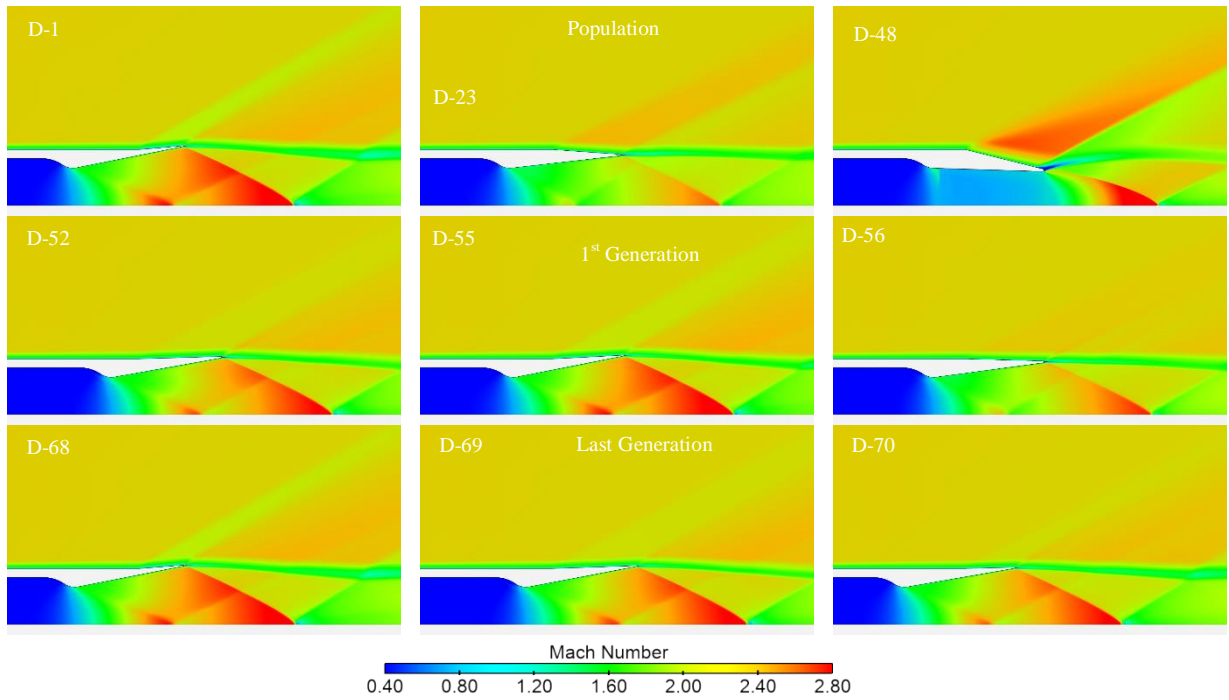


Figure 14: Mach Contours for certain Design Points

Geometry Parameters	Baseline	Best Alternative
Beta(deg)	185	178.5
Base Thickness(mm)	1.27	1.25
Boattail Length (mm)	91.09	67.5
Performance Parameters	Baseline	Best Alternative
CA	0.23356	0.22149
U_vel (m/s)	513	551

Table 4 : Comparison of Baseline with Best Alternative (Design Point-70)

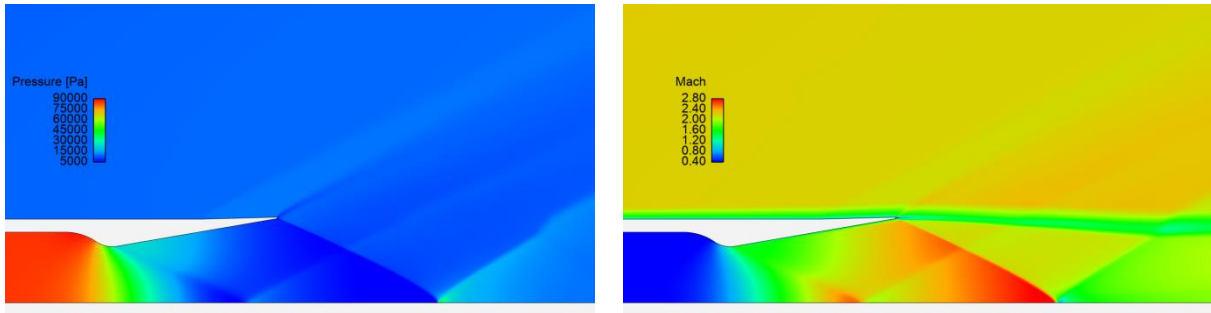


Figure 15 : Mach and Pressure Contours for Design Point-70

Design Points-70 has higher performance values, 8 % higher nozzle exit velocity and lower 5% total axial force coefficients. Model details and analysis results are shown in Table 4 and flow contours are shown in Figure 15.

4 CONCLUSIONS

In this work, missile with Putnam Nozzle is taken as a baseline for optimization cycle. Boat-tail length, base thickness and slope of rear part (β) are parameters to change exhaust geometry. With acceptable numerical method, feasible design configuration was found with the genetic algorithm with certain geometry limits.

In order to decrease elapsed time for analysis, mesh convergence is done. After that, ANSYS Fluent offers OPEN MP, IBM MPI and Intel MPI parallelization strategies. Intel MPI has 20% lower elapsed time than others. Genetic Algorithm's performs more than 70 design points to make decision to find better performance. As a result, high performance for nozzle is captured when boat-tail angle is close to zero and higher inner nozzle exit radius.

REFERENCES

- [1] Balabel, A., Hegab, A., Nasr, M., El-Behery, S.M., *Assessment of turbulence modeling for gas flow in two-dimensional convergent–divergent rocket nozzle*. Applied Mathematical Modelling 35(7), 3408– 3422 (2011).
- [2] Brown, A., M., Ruf, J., H., McDaniels, D., M., *Recovering Aerodynamic Side Loads on Rocket Nozzles using Quasi-Static Strain-Gage Measurements*, 50th Structures, Structural Dynamics, and Materials Conference, Palm Springs, California,(2009).
- [3] Castner, R. S., *Analysis of Plume Effects on Sonic Boom Signature for Isolated Nozzle Configurations*, AIAA Paper 2008-3729,(2008).
- [4] Hagemann, G., *Flow Separation and Side-Loads in Rocket Nozzles*, Paper at the 4th International Symposium Rocket Space Propulsion, Lampoldshausen, Germany,(2002).
- [5] Hamed, A., Vogiatzis, C., *Overexpanded twodimensional-convergent-divergent nozzle flow simulations, assessment of turbulence models*. Journal of Propulsion and Power 13(3), 444–445 (1997).
- [6] K. Y.Chien. *Predictions of Channel and Boundary-Layer Flows with a Low-Reynolds-Number Turbulence Model*, AIAA Journal, Vol. 20, No. 1, pp. 33-38,(1982).
- [7] L.E.Putnam and F.J.Capone. *Experimental Determination of Equivalent Solid Bodies to Represent Jets Exhausting into a Mach 2.20 External Stream*,”NASA-TN-D-5553, Dec., (1969).
- [8] Lawrence, R.A., Weynand, E.E, *Factors affecting flow separation in contoured supersonic nozzles*. AIAA Journal 6(6), 1159–1160 (1968).
- [9] R.Abid, *Evaluation of Two-Equation Turbulence Models for Predicting Transitional flows*,” Int. J.Eng Sci, Vol.31, pp.831–40,(1993).
- [10] Ostlund, J., Muhammad-Klingmann, B., *Supersonic flow separation with application to rocket engine nozzles*. Applied Mechanics Reviews 58(3), 143–177 (2005).